Spatially localized radiating diffusion flames

David Lo Jacono, Alain Bergeon, Edgar Knobloch

Spatially localized radiating diffusion flames

David Lo Jacono [a,*], Alain Bergeon [a], Edgar Knobloch [b]

[a] Institut de Mécanique des Fluides de Toulouse (IMFT), Université de Toulouse, CNRS-INPT-UPS, Toulouse, France
[b] Department of Physics, University of California, Berkeley, CA 94720, USA

A B S T R A C T

A simple model of radiating diffusion flames considered by Kavousanakis et al. (2013) [1] is extended to two spatial dimensions. A large variety of stationary spatially localized states representing the breakup of the flame front near extinction is computed using numerical continuation. These states are organized by a global bifurcation in space that takes place at a particular value of the Damköhler number and their existence is consistent with current understanding of spatial localization in driven dissipative systems.

Keywords:
Diffusion flames
Localized states
Instabilities

1. Introduction

In premixed flames, strong coupling between aerodynamics and reaction/diffusion processes arising from strong thermal expansion gives rise to Darrieus–Landau instabilities [2]. In diffusion flames, in contrast, thermal expansion plays a minor role in the thermal-diffusive processes that are behind the presence of instabilities in non-premixed flames [3]. The origin of these instabilities, which can lead to spatially uniform pulsation or to stationary or oscillating cellular structures, has been reviewed by Matalon [4,5]. Models of non-premixed flames that neglect aerodynamic effects have proved particularly useful in studies of turbulent partially premixed combustion. A well-known example is provided by the turbulent flamelet model of Peters [6] whose dynamics are dominated by diffusive processes, and not advection. The now classical flat unstrained flame introduced by Kirkbey and Schmitz [7] has been extensively studied, and numerous stability analyses [8–11] have shown that the Lewis numbers of both reactants play an essential role in selecting the nature of the possible thermal-diffusive instabilities that appear when approaching extinction (here necessarily via lean mixtures). Examples of these instabilities can be found in axisymmetric jet configurations, both experimentally [12–14] and numerically [15], as well as in tubular flames [16,17] and in unstrained flames [18,19].

The present paper is devoted to shedding additional light on the properties and dynamics of diffusion flames near flame extinction. Of particular interest in this connection is the dynamical behavior preceding extinction, including intermittency, breakup, hopping, and other types of time dependence. Diffusion flames typically exhibit cellular structures, often accompanied by temporal oscillations. Existing studies range from detailed simulations of models that retain as many of the basic processes as possible to highly simplified model systems, designed to exhibit an understanding of the qualitative properties of such flames, usually through the use of linear stability analysis in time, e.g., [20]. Such model studies are useful in developing both physical intuition and a mathematical understanding of the observed transitions. The latter often relies on bifurcation theory and relevant dynamical systems theory [1].

This paper focuses on the spatial structure of diffusion flames in the extinction regime, but goes much beyond linear stability analysis. Specifically, we show that a well-known mechanism responsible for the presence of spatially localized structures in continuous systems described by partial differential equations applies to simple models of radiating diffusion flames, and explore its consequences for the predictions of the model. This mechanism is mathematical in nature, and employs an understanding of this type of model developed using ideas based on the notion of spatial dynamics: treating the spatial profile of a stationary solution of the equations as a consequence of evolution in the spatial variable, in other words, as if space were like time [21]. This is a powerful idea that makes most sense in systems with one unbounded direction. Of course, real systems are defined by boundary-valued problems whereas time-like problems are solved with initial conditions. It turns that this difference is not crucial, and that much can be deduced based on this approach even when the domain is finite, provided it is sufficiently large. This approach is extended here to

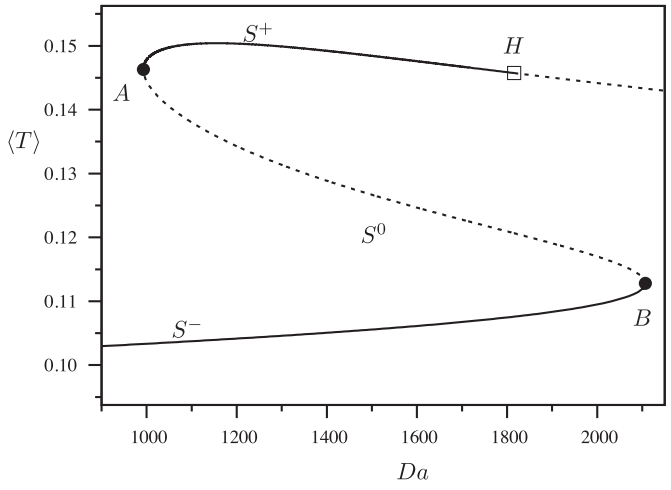

Fig. 1. The S-shaped branch of one-dimensional equilibria in terms of the average temperature $\langle T\rangle \equiv (1/2)\int_{-1}^{1}\bar{T}(x)\,dx$ as a function of the Damköhler number Da for $Le_o = Le_f = 1$, $T_b = 0.1$, $T_a = 1$ and $R = 0.2$, showing the folds A and B (solid dots) and a Hopf bifurcation at $Da \approx 1800$ (H, open square symbol) on the upper branch S^+. The labels S^0 and S^- indicate the middle and lower branches. Stable (unstable) branches are shown in solid (broken) lines.

two spatial dimensions and used to compute a large variety of stationary spatially localized states representing the breakup of the flame front near extinction. These states are organized by a global bifurcation in space that takes place at a particular value of the Damköhler number and their existence is consistent with current understanding of spatial localization in driven dissipative systems.

We consider a simple model of a radiating diffusion flame studied in [1]. Specifically, we consider a one-dimensional flame between a pair of porous walls that allow fuel (mass fraction Y_f) to diffuse in from the left ($x = -1$) and oxidizer (mass fraction Y_o) to diffuse in from the right ($x = 1$), both assumed to have the same temperature T_b. The burning process is described by a binary one step process of Arrhenius type with reaction term $w = Da\,Y_o Y_f \exp(-T_a/T)$, where T is the instantaneous temperature and the constant T_a represents the activation temperature. This temperature-activated process releases heat that is redistributed via radiation. Convection is ignored. The system is described by the nondimensional equations

$$\frac{\partial T}{\partial t} = \frac{\partial^2 T}{\partial x^2} + w - R\,Da\left(T^4 - T_b^4\right), \tag{1}$$

$$Le_o\frac{\partial Y_o}{\partial t} = \frac{\partial^2 Y_o}{\partial x^2} - w, \tag{2}$$

$$Le_f\frac{\partial Y_f}{\partial t} = \frac{\partial^2 Y_f}{\partial x^2} - w \tag{3}$$

with the boundary conditions

$$T = T_b, \quad Y_f = 1, \quad Y_o = 0 \qquad \text{at} \qquad x = -1, \tag{4}$$

$$T = T_b, \quad Y_f = 0, \quad Y_o = 1 \qquad \text{at} \qquad x = +1. \tag{5}$$

Here Le_o and Le_f are the Lewis numbers of the oxidizer and fuel, respectively, R is a parameter, and Da is the Damköhler number.

Steady solutions $(\bar{T}(x), \bar{Y}_o(x), \bar{Y}_f(x))$ of this boundary value problem are independent of Le_o, Le_f and reveal the presence of the classic S-shaped response curve as a function of the Damköhler number first identified by Liñán [22] and Peters [23]. Figure 1 shows a typical result in terms of the spatial average of the temperature, $\langle T\rangle \equiv (1/2)\int_{-1}^{1}\bar{T}(x)\,dx$, plotted as a function of Da. In the following we refer to the states on the upper branch of the curve as S^+ while those on the lower branch are labeled S^-; the states in between are labeled S^0 (Fig. 1). The stability of this solution was examined in [1] for $Le_o = Le_f = 1$. The middle segment S^0 of the S-shaped response was found to be unstable, with a real eigenvalue passing through zero at both the left and right folds, labeled A and B in Fig. 1 and represented as solid circles, as expected on the basis of standard bifurcation theory. In addition, the authors identified a sequence of Hopf bifurcations on the S^+ branch, the first of which destabilizes S^+ as Da increases (square symbol in Fig. 1), leading to temporal oscillations. Other Hopf bifurcations restabilize S^+ at larger Da (not shown), so that in all cases the large Da part of S^+ was found to be stable. This is of course the ignited state. Thus the results of [1] can be interpreted as showing that, within this model at least and for appropriate parameter values, the flame undergoes oscillations prior to extinction as Da decreases.

In this paper, we are interested in the steady solutions that bifurcate from the folds A and B on the S-shaped branch when the problem is extended to the (x, y) plane, $-\infty < y < \infty$. We refer to the y direction as the transverse direction. In other words, we study steady solutions of the problem

$$\frac{\partial T}{\partial t} = \frac{\partial^2 T}{\partial x^2} + \frac{\partial^2 T}{\partial y^2} + w - R\,Da\left(T^4 - T_b^4\right), \tag{6}$$

$$Le_o\frac{\partial Y_o}{\partial t} = \frac{\partial^2 Y_o}{\partial x^2} + \frac{\partial^2 Y_o}{\partial y^2} - w, \tag{7}$$

$$Le_f\frac{\partial Y_f}{\partial t} = \frac{\partial^2 Y_f}{\partial x^2} + \frac{\partial^2 Y_f}{\partial y^2} - w \tag{8}$$

with the y-independent boundary conditions (4)–(5) on $x = \pm 1$ and periodic boundary conditions in y with a large spatial period $L_y \gg 1$. The resulting system is spatially reversible, i.e., it is invariant under the transformation $y \to -y$. This is an important property of the model that has important consequences for the spatial eigenvalues of the base (y-invariant) state [21].

As in the one-dimensional case steady solutions of this problem are necessarily independent of the Lewis numbers Le_o, Le_f. Moreover, one class of solutions consists of those found in [1], extended uniformly in y. However, when the stability of these solutions is examined with respect to y-dependent perturbations one finds that other, y-dependent, solutions may be present. This is so despite the fact that there is no bifurcation to periodic states in the y direction, the so-called striped flames. This fact can be established by examining the linear problem for an infinitesimal perturbation $(a'(x, y, t), b'(x, y, t), c'(x, y, t))$ of the one-dimensional time-independent solution $(\bar{T}(x), \bar{Y}_o(x), \bar{Y}_f(x))$. This linear problem can be separated by writing $(a'(x, y, t), b'(x, y, t), c'(x, y, t)) = (a(x), b(x), c(x))\exp(\sigma t + iky)$. The resulting k-dependent linear problem has no solutions with zero growth rate σ when $k \neq 0$, indicating the absence of a pattern-forming Turing instability. However, when $k = 0$ the linear problem does have two locations where $\sigma = 0$. These are precisely the folds A and B on the S-shaped branch, where – as already mentioned – the stability problem for the one-dimensional solution $(\bar{T}(x), \bar{Y}_o(x), \bar{Y}_f(x))$ necessarily has a zero eigenvalue.

The paper is organized as follows. In Section 2, we provide a brief summary of the essential input from dynamical systems theory that guides our study. Detailed results are presented in Section 3 and these confirm the bifurcation structure anticipated in Section 2. The paper concludes with a brief discussion and conclusions. The numerical procedure used to compute localized structures in the present system is described in the Appendix.

2. A brief review of the theory

The theory summarized below applies to systems with a single unbounded direction such as the y direction in the present problem. We suppose that the system exhibits an S-shaped branch

of y-independent states. In this case it is known [24–26] that a branch of y-dependent solutions bifurcates from each fold, and that in both cases it does so in the inward direction. An explicit example of a weakly nonlinear calculation demonstrating this fact can be found in Appendix C of Ref. [24] or in the Appendix of Ref. [26]. The solutions that bifurcate from the folds are not periodic, but take the form of a gentle dip in S^+ (fold A) or gentle bump on top of S^- (fold B), both with y-dependent profiles of the form $a\,\mathrm{sech}^2 by$. Here $a \propto |Da - Da_{sn}|^{1/2}$ and $b \propto |Da - Da_{sn}|^{1/4}$, where Da_{sn} is the Damköhler number corresponding to fold A or B (and hence the location of the saddle-node bifurcation). Both states are reflection-symmetric with respect to the reflection $y \to -y$. With increasing distance from the fold A the dip deepens and the solution localizes in the y direction forming a state that has been called a hole: the solution connects the upper branch state S^+ to the lower branch state S^- and back again. The shape of the fronts connecting these states is determined by the value of Da and is highly nonlinear. As one follows this branch, using numerical continuation, for example, one finds that the hole broadens as the S^- state invades the domain and displaces the fronts to either side away from the center. Following the solution branch further one observes that the peak amplitude begins to decrease while the solution continues to broaden, thereby forming a peak on top of the S^- state. This process continues as one follows the branch yet further until the solution branch terminates at fold B on the branch of y-independent states. Thus the folds A and B are in fact connected by a branch of y-dependent steady solutions of problem. We refer to the resulting y-dependent solutions as localized states, and label the associated branch with the letter L. When periodic boundary conditions with a large spatial period are imposed in the y direction, as typically done in numerical computations, the above situation persists, although the bifurcations to the y-dependent states shift from the folds to nearby values of the Damköhler number. All of these transitions can be clearly seen in recent work on the Lugiato–Lefever equation arising in nonlinear optics [26]; this equation also exhibits an S-shaped response curve but the calculations are simpler since the equation as posed in [26] is one-dimensional.

The detailed behavior of the L branch depends on the nature of the spatial eigenvalues λ of $S^{\pm}$. These eigenvalues are obtained by linearizing the time-independent Eqs. (6)–(8) about the steady state $(\bar{T}(x), \bar{Y}_o(x), \bar{Y}_f(x))$ and looking for steady solutions of the form $(a'(x,y), b'(x,y), c'(x,y)) = (a(x), b(x), c(x))\exp(\lambda y)$. Because of the symmetry $y \to -y$ if λ is an eigenvalue so is $-\lambda$; if λ is complex λ^*, $-\lambda$ and $-\lambda^*$ are also eigenvalues. Thus generically spatial eigenvalues come in quartets. In particular, when the leading spatial eigenvalues (the eigenvalues whose real part is closest to zero) of $S^{\pm}$ are both real the front connecting S^+ to S^- will be monotonic, leaving S^+ along the $\lambda^+ > 0$ direction in phase space and approaching S^- along the corresponding $-\lambda^- < 0$ direction; the front at the other end of the hole will also be monotonic, leaving S^- along the $\lambda^- > 0$ direction and approaching S^+ along the $-\lambda^+ < 0$ direction. In this case the L branch is also monotonic: it extends to the right from the left fold at A and to the left from the right fold at B, becoming vertical at an intermediate Da value, hereafter Da_M, corresponding to the formation of a front between S^+ and S^-; owing to the symmetry $y \to -y$ this solution in fact corresponds to the formation of a heteroclinic cycle, when the system is viewed as evolving in y from $-\infty$ to $+\infty$. This cycle connects S^+ to S^- and back to S^+, or equivalently S^- to S^+ and back to S^-. Unfortunately all these solutions are unstable with respect to infinitesimal perturbations growing in time.

If, however, the spatial eigenvalues λ^+ of S^+ are complex the fronts will no longer be monotonic, and will exhibit growing oscillations as they depart from S^+ before approaching S^- along the $-\lambda^-$ direction. The presence of these oscillations is reflected in growing oscillations in the branch L as the hole deepens and fills with S^-. These oscillations are important because the L segments with a positive slope (i.e., between a fold on the left and the next fold on the right) in the bifurcation diagram will be stable with respect to infinitesimal perturbations in time [26]; the rest of the L branch, and in particular the segments near A and B remain unstable. Thus in this case one finds temporally stable spatially localized solutions lying on portions of the branch L – a new type of stable diffusion flame. Since the intervals of stable solutions on L lie below S^+ (see below) these spatially localized flames will be cooler than the spatially homogeneous flame S^+. Note, in particular, that these stable localized solutions are present despite the absence of spatially periodic y-dependent states. In the literature this type of behavior is known as collapsed snaking [25,27].

The above statements are consequences of the theory of spatial dynamics applied to problems of this type [21,28] and hence are not specific to the problem under discussion. In the next section, we demonstrate that these conclusions indeed apply to Eqs. (6)–(8) with the boundary conditions (4)–(5), and discuss the additional features that come about when the problem is posed on a periodic domain in the y direction with period $L_y < \infty$.

In fact the situation is yet more complex as we show in explicit computations, also in the next section.

3. Results

Our numerical results employ the same parameter values as used in [1], viz. $Le_o = Le_f = 1$, $T_b = 0.1$, $T_a = 1$ and $R = 0.2$. All calculations are performed in a domain of area $S \equiv 2 \times L_y$ with periodic boundary conditions at $y = 0, L_y$ and $L_y = 32$. We represent our results in bifurcation diagrams showing $\langle T \rangle \equiv S^{-1} \int_S T(x,y)dS$, i.e., the average temperature in the domain. This representation of the solution is preferred since it is capable of distinguishing between solutions with temperature peaks of different heights, unlike diagrams showing, for example, the maximum temperature along the center line $x = 0$. Stability properties of the solutions are determined using the Arnoldi method which is used to track the dominant temporal eigenvalues of the solutions as a function of the Damköhler number. The fact that the domain in y is finite modifies in certain respects the predictions of the general theory summarized in the preceding section, as also explained below.

3.1. Primary branches

The finite domain size $L_y < \infty$ has two main effects: (i) it forces the wavenumber k to take on integer values, and (ii) it limits, for example, the width of the S^- hole that can develop within the S^+ state. The former implies that the bifurcations at the left and right folds break up into a series of successive bifurcations generating solutions with $k = 1, 2, 3, \ldots$, with $k = 1$ representing one wavelength within the y domain, $k = 2$ representing two wavelengths etc. Since modulation of $(\bar{T}(x), \bar{Y}_o(x), \bar{Y}_f(x))$ with wavenumber $0 < k \ll 1$ is no longer possible these bifurcations will be displaced from the folds, with the bifurcation generating $k = 1$ closest to the fold, $k = 2$ further from the fold, etc. Figure 2(a) shows the S-shaped branch of y-independent solutions computed in [1] (Fig. 1) together with five branches of y-dependent states connecting the region near fold A with the region near fold B. All of these branches, hereafter L_k, behave in a similar way, with the $k = 1$ closest to the theoretically predicted behavior. Near the primary bifurcation point near B the solution corresponds to the slowly varying peak state; by the time one reaches the first fold on the left this peak state has grown in amplitude to the amplitude of the S^+ state and has self-focused into a single spatially localized pulse whose shape is determined by the value of the Damköhler number at this fold (Fig. 3, lowest panel). At this

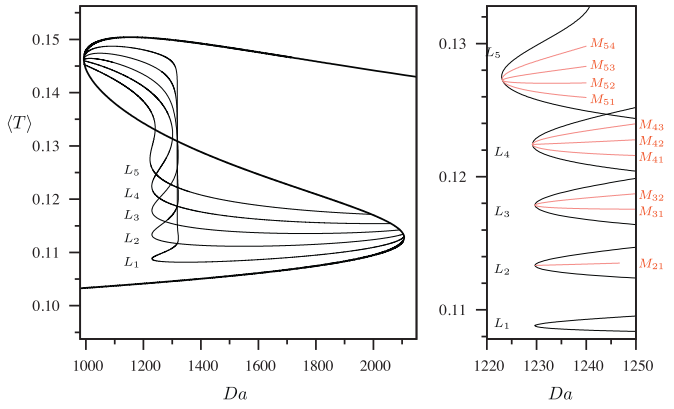

Fig. 2. (a) Bifurcation diagram showing the quantity $\langle T\rangle \equiv S^{-1}\int_S T(x,y)dS$ as a function of the Damköhler number Da for $Le_o = Le_f = 1,\ T_b = 0.1,\ T_a = 1,\ R = 0.2$ and $L_y = 32$. The branches of k-pulse localized states are denoted L_k. Stable (unstable) branches are indicated in solid (broken) lines. (b) A close-up of the left folds on each of the L_k branches shown in (a) showing the presence of tertiary branches of multipulse states of unequal height (stability not indicated).

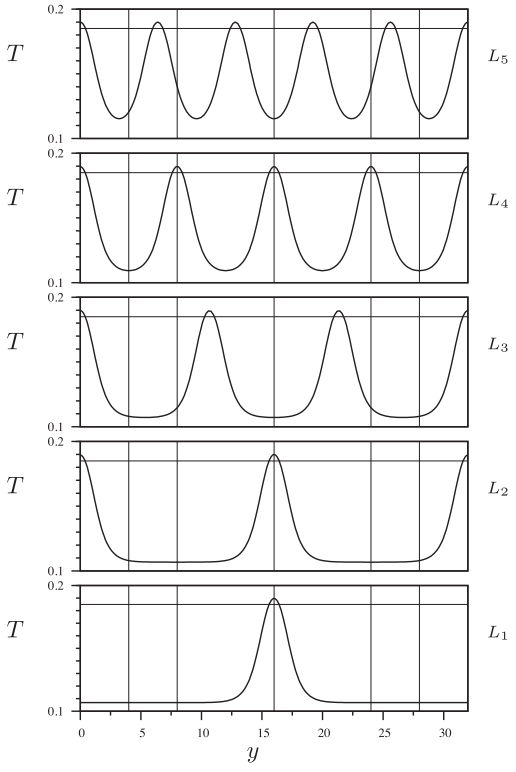

Fig. 3. Solutions $T(0, y)$ at the left folds on the L_k branches for the parameter values of Fig. 2 and appropriate values of the Damköhler number Da. The horizontal lines indicate the amplitude of the plateau corresponding to $Da = Da_M$; the vertical lines indicate the axes of symmetry of the different solutions.

fold the branch acquires stability and the pulse remains stable until the next fold on the right where it loses stability again. Since there is in fact an infinite number of oscillations in the branch as $\langle T\rangle$ increases (impossible to see on the scale of the figure) this process repeats, generating an exponentially decreasing sequence of intervals in Da with stable pulses. These successive pulses differ in the width of the plateau at amplitude S^+ that is enclosed by the oscillating fronts on either side, whose profile is fixed by the Damköhler number $Da \approx Da_M = 1318$. The other branches behave similarly, except that L_2 self-focuses into two identical equidistant pulses, L_3 self-focuses into three identical equidistant pulses, etc. The pulses comprising the L_1, L_2, $L_3, \ldots$ solutions at the first folds on the left differ only very slightly, owing to the slightly different values of Da at these folds, and this remains so provided they remain sufficiently separated. Of course, since the pulse width is determined by Da only a finite number of pulses can fit into the available y-domain. For this reason the solution branches with $k > 3$ depart from the theoretically predicted behavior: the corresponding solutions can no longer be considered to be spatially localized and significant interaction between pulses takes place. For these reasons the L_k branches with $k > 3$ no longer oscillate, and indeed do not undergo the abrupt growth in the pulse width predicted to take place near Da_M.

The value $Da = Da_M$ corresponds to the formation of a heteroclinic cycle connecting the homogeneous states S^+ and S^- at this value of Da, and plays the role of a Maxwell point familiar from systems exhibiting gradient dynamics [21]. Figure 4 shows several profiles at $Da \approx Da_M$ with increasing values of $\langle T\rangle$. At the first right fold at the lower end of the near-vertical segment of the L_1 branch the one-pulse state shown in Fig. 3 (bottom panel) starts to develop a dimple in the center (Fig. 4, profile 1). This is a consequence of the complex spatial eigenvalues of S^+. As $\langle T\rangle$ increases the pulse broadens (Fig. 4, profiles 2 and 3). In an infinite system this process continues indefinitely, resulting in the formation of the heteroclinic cycle connecting S^+ and S^-. In a domain of finite period this process inevitably terminates and the branch turns at the top towards lower Damköhler numbers. Figure 4, profile 4, shows that in this regime the minima at either end start to lift up, creating a hole-like modulation of the high temperature state S^+. With decreasing Da this hole becomes shallower and shallower and at the termination point near fold A the hole disappears and the state S^+ is recovered. Of course, because of translation invariance, the hole can be moved to the center of the periodic domain. One sees that such a state therefore represents an "anti-pulse". Thus on a finite domain the branch of pulses bifurcating from B connects to the branch of holes or anti-pulses that bifurcates from A [26]. Analogous evolution takes place along branches L_k, $k > 1$, with the same value of Da_M.

We emphasize that the oscillatory approach of the solution branches in Fig. 2(a) to $Da = Da_M$ and hence the presence of the folds on the L_k branches is a direct consequence of the fact that the leading spatial eigenvalues of the state S^+ at $Da = Da_M$ are complex. These oscillations in turn stabilize the portions of the L_k branches with positive slope and hence lead to multistability of different localized states in the vicinity of Da_M.

3.2. Secondary branches

For $k > 1$ the primary states produced by the above process resemble periodic arrays of pulses. It is therefore not surprising that the folds on these branches generate a secondary family of hole-like states, i.e., spatially *modulated* arrays of pulses. The mechanism is essentially the same, except that this time the stability problem is of Floquet type and the computation of the modulated states near the folds cannot be accomplished analytically even in one spatial dimension. Figure 2(b) shows the secondary branches near the left folds on the primary branches L_k of localized states. The modulational instability generates solutions consisting of a certain number of higher and lower peaks taken from the upper and lower branches on either side of the L_k fold. We use the integer ℓ, $\ell < k$, to denote the number of higher peaks in the solution ($k - \ell$ is then the number of lower peaks), and label the resulting modulated solutions using the notation $M_{k\ell}$. In each case we observe the presence of $k - 1$ secondary branches. In particular, when $k = 1$ there is no possible modulation, and indeed no secondary bifurcation is observed. When $k = 2$ a modulation centered on $y = 0$ can either increase or decrease the height of the central peak (Fig. 5). However, translation invariance of the system in the y

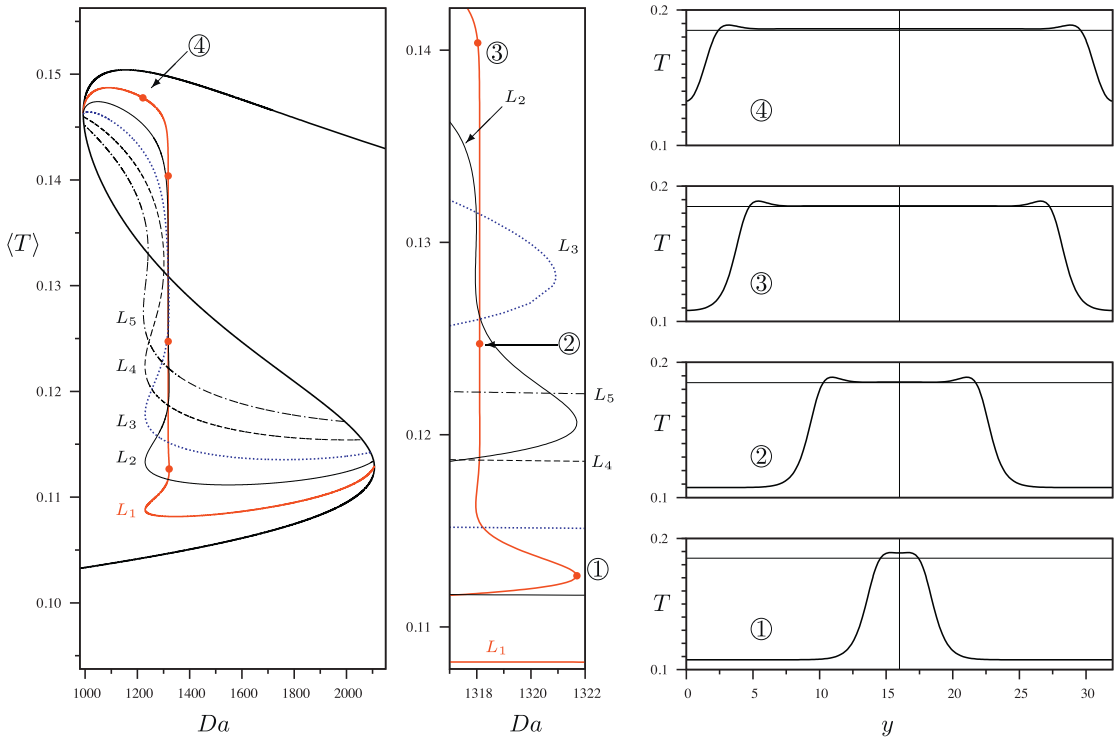

Fig. 4. Detail of Fig. 2 in the vicinity of $Da = Da_M$ showing the abrupt evolution of the solution profile that takes place in this regime. The profiles $T(0, y)$ shown on the right correspond to the numbered locations: ①: $Da = 1321.6974$, ②: $Da = 1318.1069$, ③: $Da = 1318.0387$, ④: $Da = 1221.3835$. The horizontal lines in the right panels indicate the plateau corresponding to $Da = Da_M$; the vertical lines indicate the axis of symmetry of the solutions.

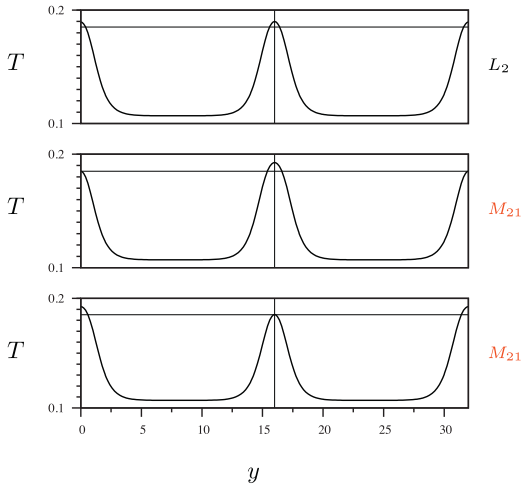

Fig. 5. Comparison of the L_2 solution (top panel) with the M_{21} solution (lower panels) at $x = 0$. The solutions in the lower panels are related by translation through $L_y/2$. The thin horizontal line connects the peaks with the smaller amplitude and is drawn to emphasize the height differences arising from spatial modulation of the L_2 state in the top panel. The Damköhler numbers are (L_2) 1229.7331, (M_{21}) 1245.8670, and (M_{21}) 1244.0886.

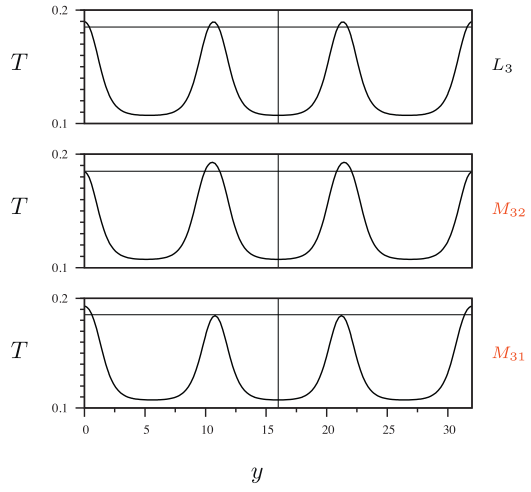

Fig. 6. Comparison of the L_3 solution (top panel) with the M_{31} and M_{32} solutions (lower panels) at $x = 0$. The Damköhler numbers are (L_3) 1229.6859, (M_{32}) 1249.4207 and (M_{31}) 1250.0697.

direction shows that the resulting two states are in fact equivalent; thus only one branch of modulated pulses, hereafter M_{21}, bifurcates from the vicinity of the left fold of the L_2 branch (Fig. 2(b)). When $k = 3$ a modulation centered on $y = 0$ can either decrease the amplitude of the two middle peaks or increase it. The resulting states are now distinct and hence two branches of secondary modulated solutions bifurcate from the vicinity of the lowest fold on the L_k branch (Fig. 6). When $k = 4$ there are three distinct secondary branches labeled M_{43}, M_{42} and M_{41} (Fig. 7), and similarly for $k = 5$ (Fig. 8). As each of these branches is followed from their birth in the direction of increasing Da, all replicate the same type of snaking in the vicinity of Da_M as the primary branches. Moreover, similar tertiary bifurcations take place at all the other folds on the L_k branches. For a similar construction in a different two-dimensional system, see [29].

The above analysis is important for the stability of the L_k states. We have already noted that the L_1 branch is initially unstable with a single unstable eigenvalue. This is because it bifurcates from S^0 above the right fold, where S^0 is once unstable. This bifurcation is supercritical, in the sense that it is in the direction of increasing instability of S^0 (decreasing Damköhler number). Consequently L_1 is once unstable. If no additional bifurcations take place L_1 will restabilize at the first fold since its eigenvalue behaves like that of

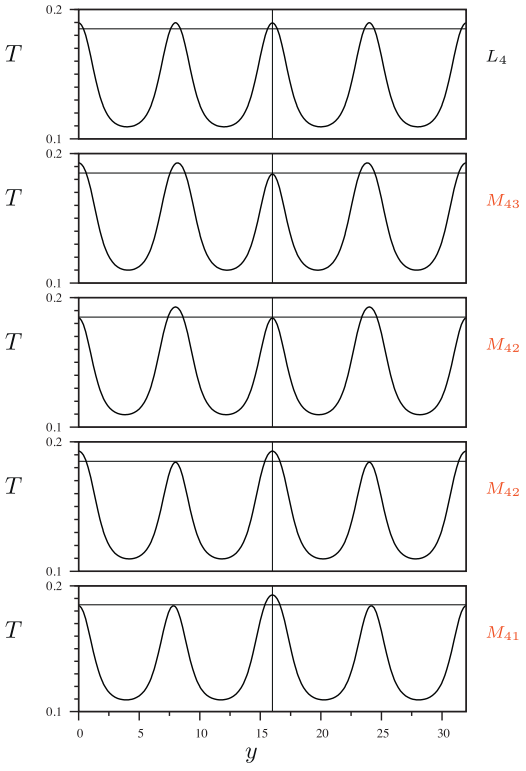

Fig. 7. Comparison of the L_4 solution (top panel) with the M_{43} solution (second panel), the M_{42} solutions (panels three and four) and the M_{41} solution (last panel), all at $x = 0$. The solutions in panels three and four are related by translation by $L_y/4$. The Damköhler numbers are (L_4) 1229.1817, (M_{43}) 1249.7594, (M_{42}) 1249.6024, (M_{42}) 1249.6946 and (M_{41}) 1249.7307.

S^0 which also restabilizes at a left fold (fold A). Thus one expects the single pulse state to be stable above the first left fold of L_1; this state is destabilized by the same eigenvalue at the next fold on the right, and so on all the way up the L_1 branch. Similarly, the branch L_2 is twice unstable near the bifurcation that creates it (it is unstable with respect to a spatially uniform eigenfunction and also with respect to single-pulse perturbations). The first of these eigenvalues restabilizes at the left fold of L_2 while the other is involved in the bifurcation to the modulated state M_{21} that takes place near this fold. Thus after these two bifurcations at or near the left fold the two-pulse state acquires stability. At the same time we see that the secondary bifurcation to the M_{21} state is subcritical, and hence this state is unstable near the bifurcation that creates it (Fig. 2(b)). By the same argument the three-pulse state L_3 also acquires stability after the left fold on L_3 and the two successive bifurcations creating M_{31} and M_{32}, etc. These results are completely consistent with our numerical continuation results.

4. Discussion and conclusions

In this paper, we have examined a simple model of diffusive flames with radiative temperature redistribution, focusing on its properties near the extinction regime (fold labeled A). Despite its simplicity the model exhibits interesting properties. Using numerical branch-following methods, motivated by a theoretical understanding of the origin of spatially localized structures [21], we identified a sequence of branches consisting of k equidistant temperature peaks along the flame front. These solutions represent states generated by the breakup of the front, and correspond to cooler structures centered on the middle of the channel ($x = 0$) and localized in the transverse direction. We have seen that these states are located near the "Maxwell" point $Da = Da_M$ corresponding to the appearance of a heteroclinic connection between the cold homogeneous state and the homogeneous flame, and that they can be stable provided the spatial eigenvalues of the hot homogeneous state are complex. We have confirmed that this is indeed the case for the parameter values considered in [1].[1] Applying the same ideas to the localized states L_k, now viewed as periodic states with period L_y, we discovered the presence of multiple tertiary branches originating from the vicinity of all folds on the L_k branches, and consisting of k peaks of different heights. Although we did not determine the stability properties of these tertiary states we have argued that their presence is in fact key for the stability of the multipulse states L_k, $k > 1$, since bifurcations to these states are required to stabilize the multipulse states near

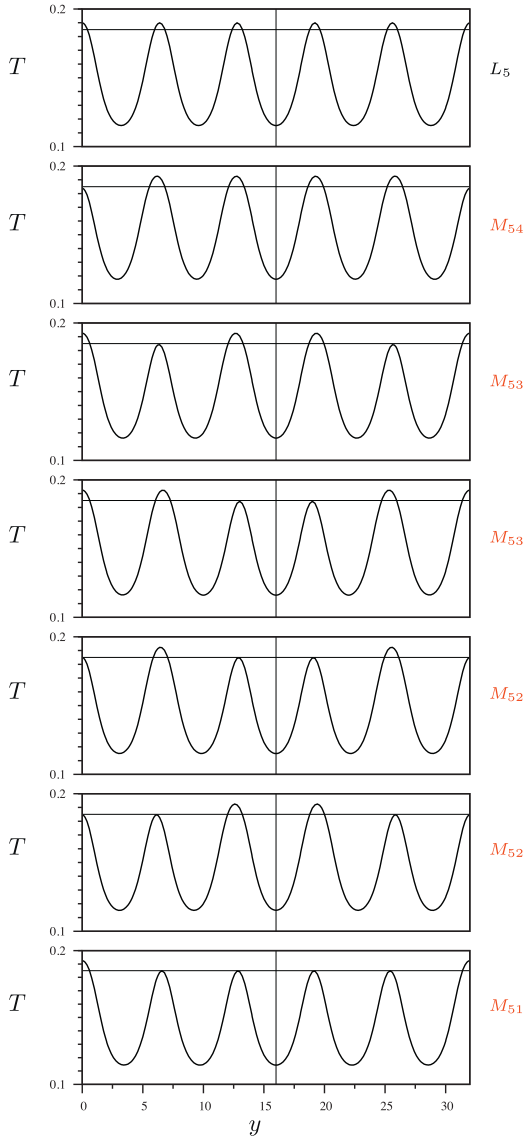

Fig. 8. Comparison of the L_5 solution (top panel) with the M_{54} solution (second panel), two distinct M_{53} solutions (panels three and four), two distinct M_{52} solutions (panels five and six), and one M_{51} solution (panel seven). The branches of the M_{52} and of the M_{53} solutions are distinct but coincide in the representation used to plot them, to within numerical error. The Damköhler numbers are (L_5) 1222.9785, (M_{54}) 1239.7467, (M_{53}) 1239.7574, (M_{53}) 1239.3069, (M_{52}) 1238.0365, (M_{52}) 1239.8294 and (M_{51}) 1239.7314.

[1] These eigenvalues become pure imaginary at and beyond the Hopf bifurcation identified in [1] since S^+ is then unstable in *time*, cf. [25].

$Da = Da_M$. These results suggest a simple procedure for identifying the location in parameter space where localized flames are present – it suffices to compute the dependence of Da_M on the model parameters and use the result to track Da_M through parameter space.

We remark that each of our L_k solutions corresponds to a periodic state on the real line, $-\infty < y < \infty$, each with a different basic wavelength. Each of these periodic states undergoes a fold on the left much like the much-studied Swift–Hohenberg equation with a quadratic-cubic nonlinearity [30]. It follows that a pair of branches of spatially localized *pulse trains* necessarily bifurcates from the left fold of such replicated L_k states and that these undergo homoclinic snaking as described in [21,28], in contrast to the collapsed snaking exhibited by L_k. Thus on large domains, admitting modulation extending over many wavelengths, a yet greater variety of localized structures, consisting of coexisting groups of pulses with different numbers of pulses, can be found. However, the corresponding calculations appear prohibitive and we have not pursued this direction further.

The model studied here, despite its simplicity, captures the essential qualitative properties of "real" diffusive flames seen in experiments. To demonstrate that this is so a movie is presented as supplemental material. This movie records an experiment in the first version of a novel one-dimensional burner [18]. The experiment consists of a closed square combustion chamber with the reactants *and products* positioned in a counterflow configuration. This is done using 625 injection needles (1 mm O.D.) through which the reactant is fed in while the hot air/products exit the chamber inbetween the needles. The oxidizer mixture (O_2–CO_2) for this movie was fixed at 70% O_2 by volume (62.92% mass), with the reactant mixture (H_2–CO_2) slowly decreasing from 24% to 12% H_2 by volume (1.41% to 0.73% mass). The flow rate was maintained at $Q_o = 3.33 \times 10^{-5}$ m^3/s (33.3 ml/s), $Q_f = 3.00 \times 10^{-5}$ m^3/s (30 ml/s) with a cross-sectional area of 46 mm^2. The movie was captured by a digital camcorder (Sony, DSR 300P), at an oblique angle of about 45° with respect to the flat and horizontal flame. Frames from this movie are shown as still pictures in [18]. The movie illustrates the transition process from a flat flame to a fully cellular flame all the way to spatially localized flamelets. The movie begins with a flat flame, and as the reactant mixture becomes poorer in H_2 cell formation starts at the flame edges adjacent to the chamber walls. We note the cells are not spatially locked to the tube grid. As the H_2 concentration is reduced further, the cellular region grows towards the center of the flame. After some time (around 1 min), the entire flame consists of cells and the transition to the fully cellular regime is considered complete. At this point, the cell structures (flame "patches") are not stationary. As the H_2 concentration is reduced even further, the number of cells progressively decreases until the extinction limit is reached. We believe that the flame undergoes breakup into spatially localized structures in the time interval 1.0–1.5 min. It is in this region that our insight into the presence of a large multiplicity of localized structures with a specific characteristic size becomes particularly relevant.

The key new observation for near-extinction flame dynamics is the observation that the fold A representing extinction of the uniform (y-invariant) flame is responsible for the presence of a large number of simultaneously stable spatially localized flames at nearby values of the Damköhler number. We believe that this property carries over to more sophisticated models and hence has broad relevance to diffusion flames in general. This new class of states becomes particularly relevant when the uniform flame S^+ becomes unstable to oscillations already near A, for example, by moving the Hopf bifurcation H in Fig. 1 to lower values (by changing the value of the parameter R or the Lewis numbers Le_o, Le_f) so that the localized flames are also time-dependent.

Given the success of our approach it is now of considerable interest to explore extensions of the model to more realistic configurations. In future work we shall explore the effects of different fuel and oxidizer Lewis numbers on the dynamical properties of the localized states we have found (which are independent of Le_o, Le_f), as well as including the effects of hydrodynamic flow (cf. [20]), and extending the calculations to three dimensions in order to identify spot-like flames in the extinction region. More realistic models should also include density dependence of the model parameters.

Acknowledgment

The work of EK was supported in part by the National Science Foundation under grant DMS-1211953.

Appendix

In order to compute steady solutions of Eqs. (6)–(8) with the boundary conditions (4)–(5) as a function of the Damköhler number Da, we use a standard numerical arclength continuation method [31] based on a Newton solver for the time-independent version of the equations [32]. This methods allows one to follow branches of stable or unstable steady states, compute their linear stability, locate secondary bifurcations and follow the resulting secondary solution branches.

To do so, the equations are spatially discretized using a spectral element method in which the domain $[0, 2] \times [0, L_y]$ is decomposed into N_e spectral elements of size $[0, 2] \times [kl_y, (k+1)l_y]$ with $N_e l_y = L_y$ and $0 \le k \le N_e - 1$. In each element, the fields (T, Y_o, Y_f) are approximated by a high-order interpolant through $n_x \times n_y$ Gauss–Lobatto–Legendre points. In the continuation procedure, the solutions are calculated as a function of the branch arclength. Each point of this branch corresponds to a steady state that includes the values $\bar{Y} \equiv (\bar{T}_j, \bar{Y}_{oj}, \bar{Y}_{fj})_{1 \le j \le N}$ of (T, Y_o, Y_f) at the $N = N_e n_x n_y$ discretization points and the corresponding Damköhler number Da. The unknowns $\bar{X} \equiv (\bar{Y}, Da)$ are obtained by solving the discretized steady state equations by a Newton method. The arclength is then incremented and the procedure repeated.

The Newton solver that we use derives from a first-order time integration scheme for the time-dependent problem [33,34] and we use a scheme in which the diffusive linear part of the equations is treated implicitly while the nonlinear part is treated explicitly. Each time step requires the inversion of three Helmholtz problems. The discrete version of the weak form of each Helmholtz problem is first transformed into a set of n_x one-dimensional problems after a partial diagonalization of the operator, each of which is solved using a Schur decomposition method.

Once a steady state is obtained, its linear stability properties are studied by means of Arnoldi's method. This method allows one to compute the most unstable eigenvalues and the corresponding eigenvectors, and these can be used to locate secondary bifurcations. Once a steady bifurcation is located, the corresponding unstable eigenvector and associated steady state are used to build a predictor for a solution along the emerging branch; the code then uses continuation to follow the new branch. Again, the implementation of the Arnoldi procedure uses the first order time-stepping code following the procedure originally proposed by Tuckerman [33].

The technique has been used with success to compute time-independent localized structures in several systems arising in fluid mechanics [35–38].

Supplementary material

Supplementary material associated with this article can be found, in the online version, at 10.1016/j.combustflame.2016.10.002.

References

[1] M.E. Kavousanakis, L. Russo, F.S. Marra, C. Siettos, Homoclinic bifurcations in radiating diffusion flames, Combust. Theory Modell. 17 (1) (2013) 40–52.
[2] G.I. Sivashinsky, Instabilities, pattern formation, and turbulence in flames, Annu. Rev. Fluid Mech. 15 (1983) 179–199.
[3] M. Matalon, P. Metzener, The effect of thermal expansion on diffusion flame instabilities, J. Fluid Mech. 647 (2010) 453–472.
[4] M. Matalon, Intrinsic flame instabilities in premixed and nonpremixed combustion, Annu. Rev. Fluid Mech. 39 (2007) 163–191.
[5] M. Matalon, Flame dynamics, Proc. Combust. Inst. 32 (2009) 57–82.
[6] N. Peters, Laminar flamelet concepts in turbulent combustion, Symp. (Int.) Combust. 21 (1) (1986) 1231–1250.
[7] L.L. Kirkbey, R.A. Schmitz, An analytical study of stability of a laminar diffusion flame, Combust. Flame 10 (3) (1966) 205–220.
[8] J.S. Kim, F.A. Williams, P.D. Ronney, Diffusional-thermal instability of diffusion flames, J. Fluid Mech. 327 (1996) 273–301.
[9] S. Cheatham, M. Matalon, A general asymptotic theory of diffusion flames with application to cellular instability, J. Fluid Mech. 414 (2000) 105–144.
[10] H.Y. Wang, J.K. Bechtold, C.K. Law, Nonlinear oscillations in diffusion flames, Combust. Flame 145 (1–2) (2006) 376–389.
[11] P. Metzener, M. Matalon, Diffusive-thermal instabilities of diffusion flames: onset of cells and oscillations, Combust. Theory Modell. 10 (4) (2006) 701–725.
[12] M. Füri, P. Papas, P.A. Monkewitz, Non-premixed jet flame pulsations near extinction, Proc. Combust. Inst. 28 (2000) 831–838.
[13] D. Lo Jacono, P. Papas, P.A. Monkewitz, Cell formation in non-premixed, axisymmetric jet flames near extinction, Combust. Theory Modell. 7 (4) (2003) 635–644.
[14] D. Lo Jacono, P.A. Monkewitz, Scaling of cell size in cellular instabilities of non-premixed jet flames, Combust. Flame 151 (1–2) (2007) 321–332.
[15] A.L. Valär, C.E. Frouzakis, P. Papas, A.G. Tomboulides, K. Boulouchos, Three-dimensional simulations of cellular non-premixed jet flames, Combust. Flame 157 (4) (2010) 653–666.
[16] S. Hu, P.W. Pitz, Y. Wang, Extinction and near-extinction instability of non-premixed tubular flames, Combust. Flame 156 (2009) 90–98.
[17] S.W. Shopoff, P. Wang, R.W. Pitz, Experimental study of cellular instability and extinction of non-premixed opposed-flow tubular flames, Combust. Flame 158 (11) (2011) 2165–2177.
[18] D. Lo Jacono, P. Papas, M. Matalon, P.A. Monkewitz, An experimental realization of an unstrained, planar diffusion flame, Proc. Combust. Inst. 30 (2005) 501–509.
[19] E. Robert, P.A. Monkewitz, Thermal-diffusive instabilities in unstretched, planar diffusion flames, Combust. Flame 159 (3) (2012) 1228–1238.
[20] R. Vance, M. Miklavcic, I.S. Wichman, On the stability of one-dimensional diffusion flames established between plane, parallel, porous walls, Combust. Theory Modell. 5 (2) (2001) 147–161.
[21] E. Knobloch, Spatial localization in dissipative systems, Annu. Rev. Cond. Matter Phys. 6 (2015) 325–359.
[22] A. Liñan, The asymptotic structure of counterflow diffusion flames for large activation energies, Acta Astronautica 1 (7–8) (1974) 1007–1039.
[23] N. Peters, Laminar diffusion flamelet models in non-premixed turbulent combustion, Prog. Energy Combust. Sci. 10 (3) (1984) 319–339.
[24] J. Burke, A. Yochelis, E. Knobloch, Classification of spatially localized oscillations in periodically forced dissipative systems, SIAM J. App. Dyn. Syst. 7 (3) (2008) 651–711.
[25] Y.-P. Ma, J. Burke, E. Knobloch, Defect-mediated snaking: A new growth mechanism for localized structures, Phys. D: Nonlinear Phenomena 239 (19) (2010) 1867–1883.
[26] P. Parra-Rivas, E. Knobloch, D. Gomila, L. Gelens, Dark solitons in the Lugiato–Lefever equation with normal dispersion, Phys. Rev. A 93 (2016) 063839.
[27] J. Knobloch, T. Wagenknecht, Homoclinic snaking near a heteroclinic cycle in reversible systems, Phys. D: Nonlinear Phenomena 206 (1–2) (2005) 82–93.
[28] J. Burke, E. Knobloch, Homoclinic snaking: structure and stability, Chaos 17 (2007) 037102.
[29] I. Mercader, O. Batiste, A. Alonso, E. Knobloch, Convectons, anticonvectons and multiconvectons in binary fluid convection, J. Fluid Mech. 667 (2011) 586–606.
[30] J. Burke, E. Knobloch, Localized states in the generalized Swift-Hohenberg equation, Phys. Rev. E 73 (2006) 056211.
[31] R. Seydel, Practical bifurcation and stability analysis: From equilibrium to chaos, Springer-Verlag, New York, 1991.
[32] H.A. Dijkstra, F.W. Wubs, A.K. Cliffe, E. Doedel, I.F. Dragomirescu, B. Eckhardt, A.Y. Gelfgat, A.L. Hazel, V. Lucarini, A.G. Salinger, E.T. Phipps, J. Sanchez-Umbria, H. Schuttelaars, L.S. Tuckerman, U. Thiele, Numerical bifurcation methods and their application to fluid dynamics: analysis beyond simulation, Commun. Comput. Phys. 15 (2014) 1–45.
[33] L.S. Tuckerman, Steady-state solving via Stokes preconditioning; Recursion relations for elliptic operators, in: D.L. Dwoyer, M.Y. Hussaini, R.G. Voigt (Eds.), Proceedings of the 11th International Conference on Numerical Methods in Fluid Dynamics, Springer-Verlag, Berlin, 1989, pp. 573–577.
[34] C.K. Mamun, L.S. Tuckerman, Asymmetry and Hopf bifurcation in spherical Couette flow, Phys. Fluids 7 (1995) 80–91.
[35] A. Bergeon, E. Knobloch, Periodic and localized states in natural doubly diffusive convection, Phys. D: Nonlinear Phenomena 237 (2008) 1139–1150.
[36] D. Lo Jacono, A. Bergeon, E. Knobloch, Spatially localized magnetoconvection, Fluid Dyn. Res. 44 (2012) 031411.
[37] C. Beaume, A. Bergeon, H.-C. Kao, E. Knobloch, Convectons in a rotating fluid layer, J. Fluid Mech. 717 (2013) 417–448.
[38] C. Beaume, A. Bergeon, E. Knobloch, Convectons and secondary snaking in three-dimensional natural doubly diffusive convection, Phys. Fluids 25 (2013) 024105.